Assessment of the impact of FORMOSAT-7/COSMIC-2 GNSS RO observations on mid- and low-latitude ionosphere specification and forecasting using Observing System Simulation Experiments

Chih-Ting Hsu[1,2,3], Tomoko Matsuo[2,3], Xinan Yue[4], Tzu-Wei Fang[3], Timothy Fuller-Rollew[3] and Jann-Yenq Liu[1]

[1] Institute of Space Science, National Central University, Taoyuan, Taiwan [2] Aerospace Engineering Sciences, University of Colorado at Boulder, CO, U. S. A.

[3] Space Weather Prediction Center, National Oceanic and Atmospheric Administration, Boulder, CO, USA. [4]Chinese Academy of Sciences, China

1. Introduction

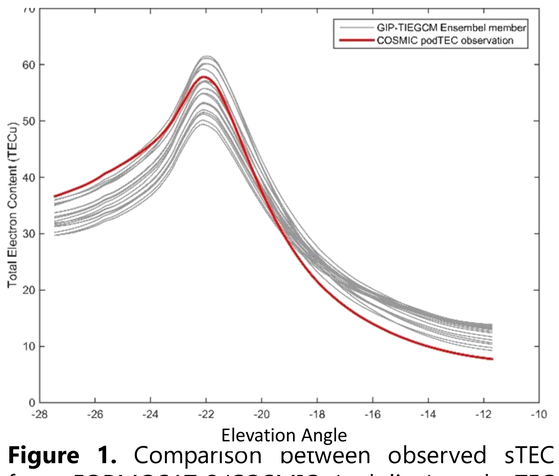

Figure 1. Comparison between observed sTEC from FORMOSAT-3/COSMIC (red line) and sTEC calculated from GIP/TIEGCM ensembles (grey lines).

Motivations and Goals

The Formosa Satellite-7/Constellation Observing System for Meteorology, Ionosphere and Climate-2 (FORMOSAT-7/COSMIC-2) GNSS Radio Occultation (RO) payload can provide global observations of slant Total Electron Content (sTEC) with unprecedentedly high spatial and temporal resolution.

This presentation will demonstrate **(A) how the Ensemble Square Root Filter (EnSRF) [Whitaker and Hamill, 2001] can be used to assimilate sTEC observations effectively**, and **(B) impacts of FORMOSAT-7/COSMIC-2 GNSS RO data on low- and mid-latitude ionospheric specification and forecasting**.

Data assimilation system

Synthetic RO sTEC data are assimilated into a coupled model of thermosphere, ionosphere, and plasmasphere by using EnSRF.

Data - RO sTEC

- RO sTEC along a given radio path can be retrieved from signals received LEO GPS receiver
- RO path for a given sTEC can traverse through a large distance in the ionosphere and plasmasphere (up to 6000-7000 km).

Model –GIP/TIEGCM

Global-Ionosphere-Plasmasphere/Theremosphere-Ionosphere-Electrodynamics General Circulation Model (GIP/TIEGCM) [Pedatella et al, 2011] is made of following two models.

- TIEGCM – thermosphere ~ 400 - 800 km
- GIP – ionosphere and plasmasphere ~ 19000 km

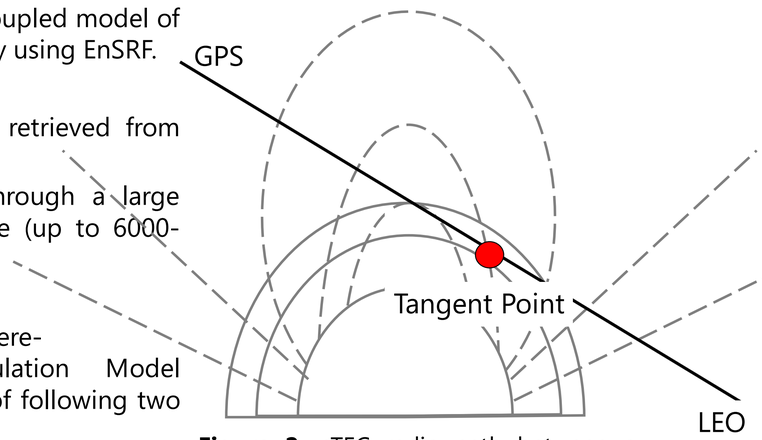

Figure 2. sTEC radio path between a LEO satellite and a GPS satellite and GIP/TIEGCM coordinates.

2. EnSRF Experiments

EnSRF sTEC Data Assimilation

Step 1 calculate the increment of observed state variable

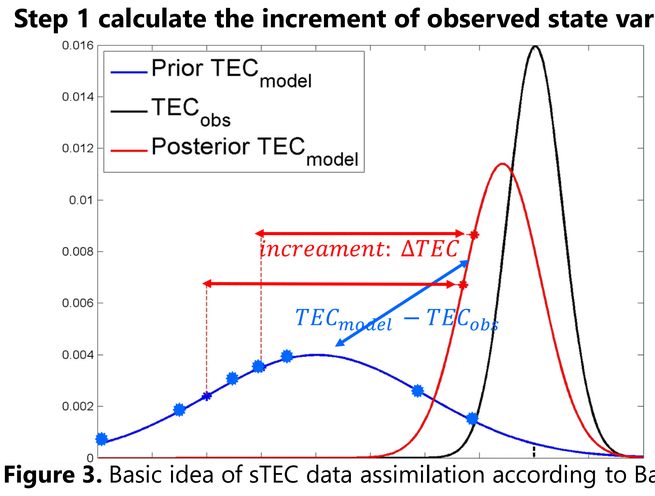

Figure 3. Basic idea of sTEC data assimilation according to Bayes rule.

Step 2 calculate the increment of model state variables

Analysis increment of state "Electron and oxygen ion density on model grid"

Regression coefficient estimated from model ensemble

$$\Delta x = \alpha \hat{b} \Delta y$$

Localization

Analysis Increment of observed variable "sTEC"

A1. Experiments with Different Ensemble Sizes

Observing System Simulation Experiments (OSSEs) with **10, 20, 30, 50** GIP/TIEGCM ensemble members are carried out.

- Synthetic sTEC data sampled from a "true" state are assimilated into the model continuously from UT 0000 to UT 1200.
- Both e^- and O^+ density are updated by using EnSRF.
- GIP/TIEGCM ensembles are generated by perturbing following model drivers according to a normal distribution specified below.

	F10.7 ($\frac{WHz}{m^2}$)	cross-tail potential drop (kV)	auroral hemispheric power (GW)
Ensemble Mean	120×10^{-22}	45	16 GW
Standard Deviation of Ensemble	15×10^{-22}	5 kV	2 GW
"True" simulation	140×10^{-22}	50 kV	18 GW

Results A1: Experiments with larger size of ensemble shows smaller RMSE because the estimation of $\hat{b}$ is better.

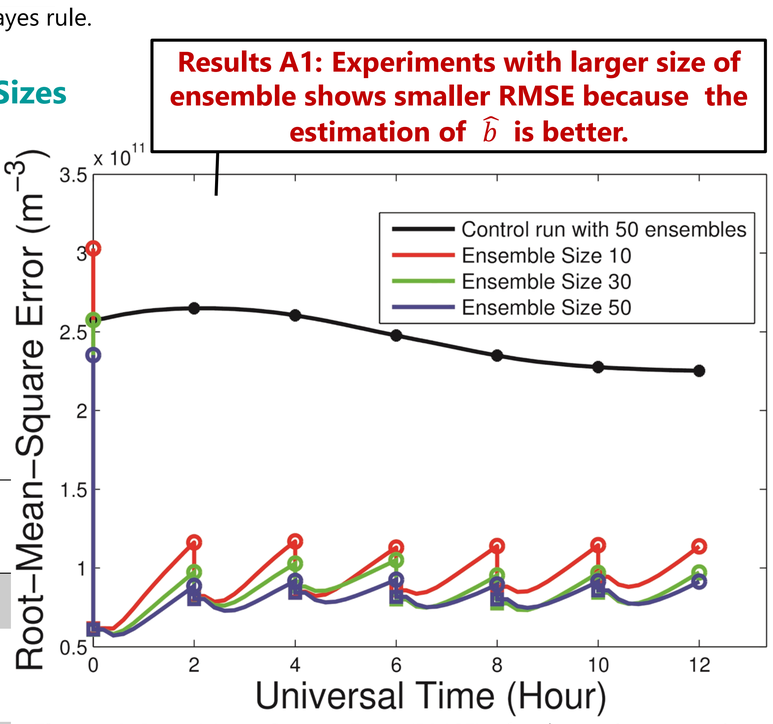

Figure 4. Root-Mean-Square Error (RMSE) of O^+ density over mid- and low- latitude F-region (-46° to 46° latitude and 200 to 500 km altitude) during data assimilation cycle.

A2. Experiments with Different Localization Length Scales

OSSEs with different localization length scales are carried out.

- Single sTEC data is assimilated into the model. The tangent point of this data is at local noon, 350 km, 0° longitude, and 0° latitude.
- Gaspari-Cohn (GC) function [Gaspari and Cohn, 1999] is used to specify α for a given normalized distance r. The tangent point is assumed as the observation location.

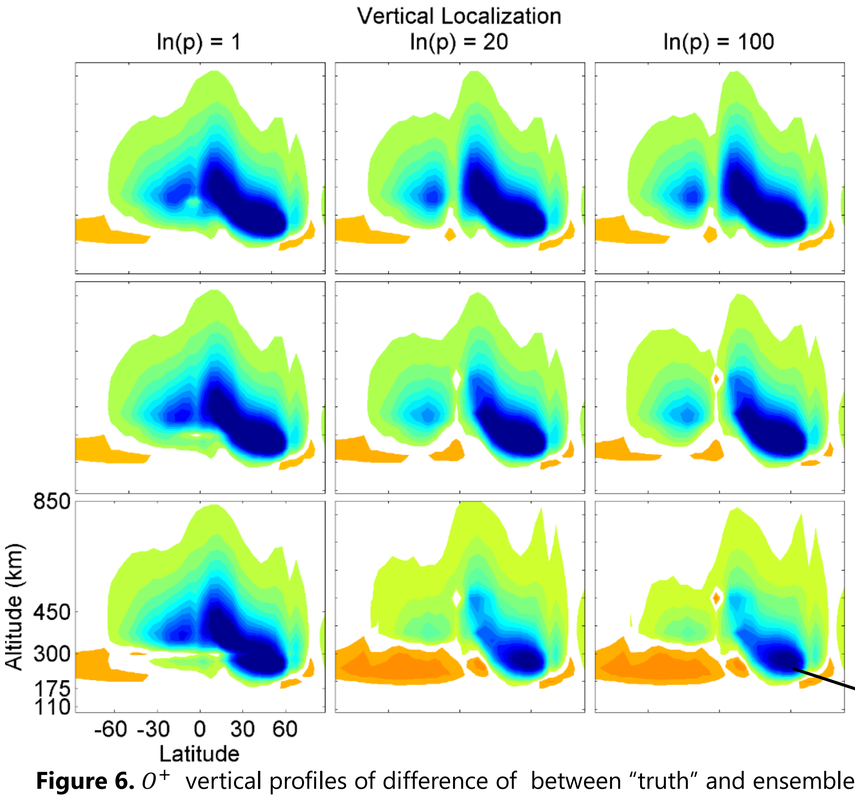

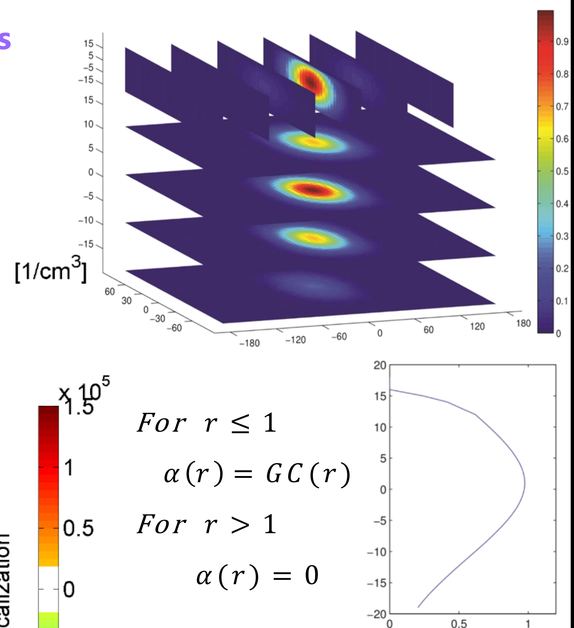

$$For\ r \le 1 \quad \alpha(r) = GC(r)$$

$$For\ r > 1 \quad \alpha(r) = 0$$

Figure 5. Top panel is the 3-D structure of GC function. Bottom panel is the GC vertical cross section

Result A2: The larger the localization length scale, the lager/smaller the E-/F-region error.

Figure 6. O^+ vertical profiles of difference of between "truth" and ensemble mean.

3. Experiments with F-3/C vs F-7/C-2

OSSEs of FORMOSAT-3/COSMIC (F-3/C) and FORMOSAT-7/COSMIC-2 (F-7/C-2) are compared with one-hour data window. An additional experiments with 24-minute data window for FORMOSAT-7/COSMIC is carried out.

	F3/C	F-7/C-2
Number of satellites	6 microsatellites	12 microsatellites - 6 low inclination satellites (Phase1) - 6 high inclination satellites(Phase2) **Only synthetic data for Phase1 are used in our experiments!**
Number of RO events per day	~ 2000 RO events per day	~ 8000 RO events per day (Phase1) [Yue et al., 2014]

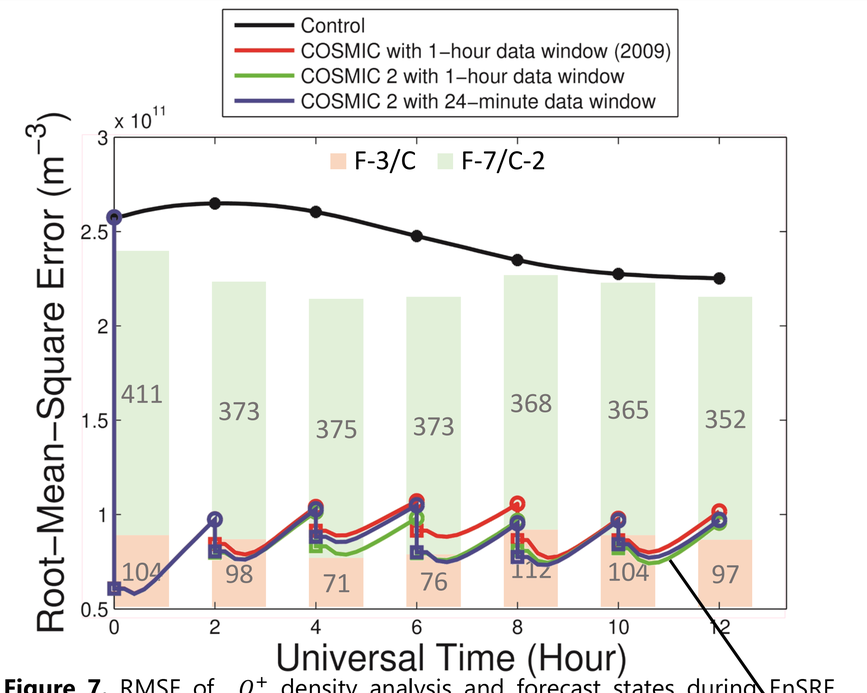

Figure 7. RMSE of O^+ density analysis and forecast states during EnSRF cycling . Light green and orange bars show the number of RO events.

New Finding: RMSEs continue decrease during forecast steps after data assimilation update likely due to T-I coupling.

Results B: With the help of F-7/C-2 sTEC data, NmF2 errors at mid- and low- latitudes are reduced significantly.

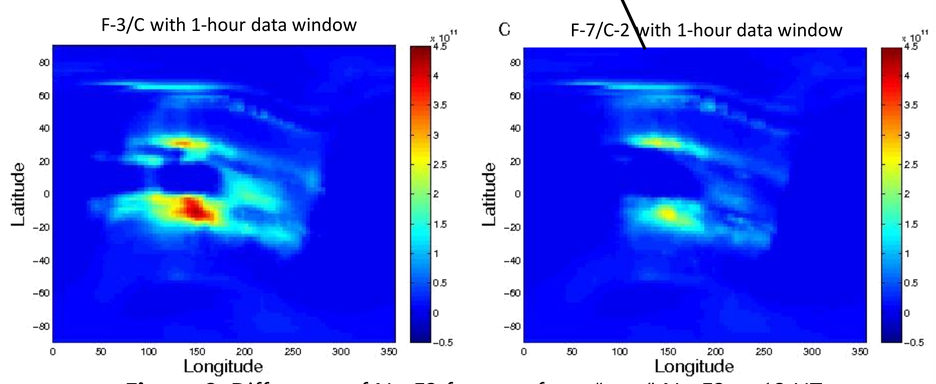

Figure 8. Difference of NmF2 forecast from "true" NmF2 at 12 UT.

4. Conclusions

A number of OSSEs are carried out for FORMOSAT-7/COSMIC-2 sTEC observations using the EnSRF.

Our main findings are as follows.

A1. EnSRF analyses and forecasts in the mid- and low-latitude F-region ionosphere improve with increasing size of ensemble.

A2. EnSRF benefits from covariance localization with a large localization length scale in E-region and a small localization length scale in F-region.

B. sTEC data from FORMOSAT-7/COSMIC-2 Phase1 have a great potential to improve the mid-and low-latitude ionospheric specification and forecast over FORMOSAT-3/COSMIC.

Furthermore, we find that the ionospheric forecast errors continue to decrease during forecast cycles of EnSRF for about 30 minutes before stating to increase. This suggests the thermosphere states influenced by updated O+ have positive effects on ionospheric forecasting.

References

Gaspari, G., and S. E. Cohn, (1999) Construction of correlation functions in two and three dimensions. *Quart. J. Roy. Meteor. Soc.*, **125**, 723–757`

Pedatella, N. M., J. M. Forbes, A. Maute, A. D. Richmond, T.-W. Fang, K. M. Larson, and G. Millward (2011), Longitudinal variations in the F region ionosphere and the topside ionosphere-plasmasphere: Observations and model simulations, *J. Geophys. Res.*, 116, A12309.

Yue, X., W. S. Schreiner, N. Pedatella, R. A. Anthes, A. J. Mannucci, P. R. Straus, and J.-Y. Liu (2014), Space Weather Observations by GNSS Radio Occultation: From FORMOSAT-3/COSMIC to FORMOSAT-7/COSMIC-2, Space Weather, 12, 616–621, doi:10.1002/ 2014SW001133.

Whitaker J. S., and T. M. Hamill (2001), Ensemble Data Assimilation without Perturbed Observations, *Mon. Wea. Rev.*, 130, 1913-1924.